

# High-Accuracy, Implicit Solution of the Extended-MHD Equations using High- Continuity Finite Elements

Stephen C. Jardin

In collaboration with  
the M3D group  
and the  
SciDAC Center for Extended MHD Modeling

**Princeton University**  
**Plasma Physics Laboratory**

Nov 18, 2004

APS, DPP Meeting

Savannah, GA

# The Center for Extended Magnetohydrodynamic Modeling

(Global Stability of Magnetic Fusion Devices)

*S. Jardin—lead PI*

*a SciDAC activity...  
Partners with:  
TOPS  
TSTT  
APDEC*

**MIT:** D. Brennan, L. Sugiyama, J. Ramos

**NYU:** B. Hientzsch, H. Strauss

**PPPL:** J. Breslau, J. Chen, G. Fu, S. Klasky, W. Park, R. Samtaney

**SAIC:** D. Schnack, A. Pankin

**TechX\*:** S. Kruger

**U. Colorado:** S. Parker, D. Barnes

**U. Utah:** A. Sanderson

**U. Wisconsin:** J. Callen, C. Hegna, C. Sovinec, C. Kim

**Utah State:** E. Held



# Considerations for a next-generation nonlinear MHD code for Magnetic Fusion Applications

i.e.: what have we learned?

- 2-fluid terms (Extended MHD) are essential to model real fusion experiments...but best form is uncertain
- Highly implicit treatment is needed to address long timescales
- There are advantages to using the potential/stream function form of the vector fields...avoids spec. pol.+ low order subsets
- High-order (4<sup>th</sup> or more) finite elements are essential for describing highly anisotropic heat conduction.
- Direct sparse matrix inversions (vs iterative solvers) in the poloidal plane can be very efficient for the MHD system
- It is advantageous to have a fast linear option to scope runs
- Boundary conditions should be applied at infinity, but we need the capability to model a nearby resistive conducting structure

# Our center is comparing 5+ different Extended-MHD models and need to be able to change models without major code restructuring

Model	Momentum Equation	Ohm's law	Whistlers <sup>1</sup>	KAW <sup>2</sup>	GV <sup>3</sup>	Slow dynamics <sup>4</sup>
General	$mn \frac{d\mathbf{V}}{dt} = -\nabla(p_e + p_i)$ $+\mathbf{J} \times \mathbf{B} - \nabla \cdot (\Pi_{\parallel e} + \Pi_{\parallel i}) - \nabla \cdot \Pi_i^{gv}$	$\mathbf{E} = -\mathbf{V} \times \mathbf{B} + \eta \mathbf{J}$ $+ \frac{1}{ne} (\mathbf{J} \times \mathbf{B} - \nabla p_e - \nabla \cdot \Pi_{\parallel e})$	Yes	Yes	Yes	Either
Generalized Hall MHD <sup>5</sup>	$mn \frac{d\mathbf{V}}{dt} = -\nabla(p_e + p_i)$ $+\mathbf{J} \times \mathbf{B} - \nabla \cdot (\Pi_{\parallel e} + \Pi_{\parallel i})$	$\mathbf{E} = -\mathbf{V} \times \mathbf{B} + \eta \mathbf{J}$ $+ \frac{1}{ne} (\mathbf{J} \times \mathbf{B} - \nabla p_e - \nabla \cdot \Pi_{\parallel e})$	Yes	Yes	No	No
Neoclassical-MHD	$mn \frac{d\mathbf{V}}{dt} = -\nabla(p_e + p_i)$ $+\mathbf{J} \times \mathbf{B} - \nabla \cdot (\Pi_{\parallel e} + \Pi_{\parallel i}) - \nabla \cdot \Pi_i^{gv}$	$\mathbf{E} = -\mathbf{V} \times \mathbf{B} + \eta \mathbf{J} - \frac{1}{ne} \nabla \cdot \Pi_{\parallel e}$	No	No	Yes	Yes
Generalized resistive MHD <sup>5</sup>	$mn \frac{d\mathbf{V}}{dt} = -\nabla p + \mathbf{J} \times \mathbf{B} - \nabla \cdot \Pi_{\parallel}$	$\mathbf{E} = -\mathbf{V} \times \mathbf{B} + \eta \mathbf{J}$	No	No	No	No
Generalized drift <sup>6</sup>	$mn \frac{d\mathbf{V}}{dt} = -mn \mathbf{V}_{di} \cdot \nabla \mathbf{V}_{\perp} + \nu_{gv}$ $+ nm \mu \nabla_{\perp}^2 \mathbf{V} - \nabla \cdot (\Pi_{\parallel e} + \Pi_{\parallel i})$ $- \nabla(p_e + p_i) + \mathbf{J} \times \mathbf{B}$	$\mathbf{E} = -\mathbf{V} \times \mathbf{B} + \eta \mathbf{J}^*$ $- \frac{1}{ne} [\nabla_{\parallel} p_e + \nabla \cdot \Pi_{\parallel e}]$	No	Yes	Yes	Yes

# All the MHD models beyond resistive MHD contain dispersive waves

## Resistive MHD

$$mn \frac{d\mathbf{V}}{dt} = -\nabla(p_e + p_i) + \mathbf{J} \times \mathbf{B} - \nabla \cdot (\Pi_{\parallel e} + \Pi_{\parallel i}) - \nabla \cdot \Pi_i^{gv}$$

Off-diagonal stress tensor terms lead to gyro-viscous waves

$$\frac{\partial \mathbf{B}}{\partial t} = -\nabla \times \mathbf{E}, \quad \mathbf{E} = -\mathbf{V} \times \mathbf{B} + \eta \mathbf{J} + \frac{1}{ne} (\mathbf{J} \times \mathbf{B} - \nabla p_e - \nabla \cdot \Pi_{\parallel e})$$

All these new “Extended MHD” waves have similar structure

Hall term leads to Whistler wave

Pressure gradient terms lead to Kinetic Alfvén wave

$$\frac{\partial^2 \mathbf{B}}{\partial t^2} = -\left(\frac{V_A^2}{\Omega}\right)^2 (\mathbf{b} \cdot \nabla)^2 \nabla^2 \mathbf{B}$$

Note 4<sup>th</sup> spatial derivatives

Limiting form gives wave-like equation where wave speed is inversely proportional to wavelength:

$$\text{i.e. } \frac{\omega}{k} \sim k$$

Need viable implicit techniques for these 4<sup>th</sup> order (in space) equations to provide numerical stability for large timesteps.

## Highly anisotropic heat conduction requires accurate spatial representation and implicit time differencing

$$\frac{\partial T}{\partial t} = \nabla \cdot \left[ \kappa_{\parallel} \frac{\vec{B}\vec{B}}{B^2} \cdot \nabla T \right] + \nabla \cdot \kappa \nabla T + S$$

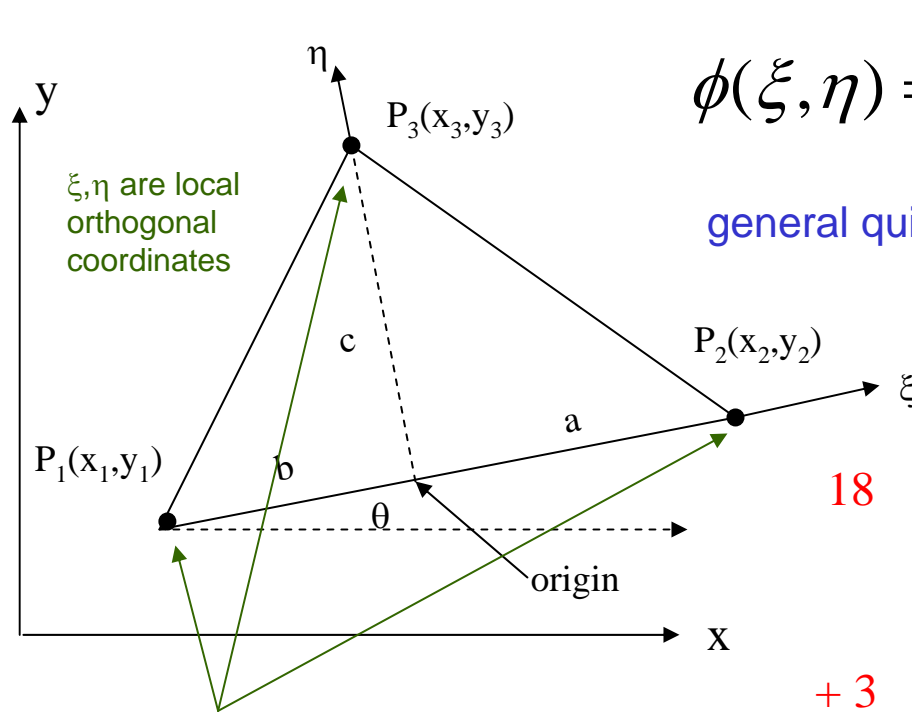
In a highly magnetized fusion plasma,  $\kappa_{\parallel} \gg \kappa$

- Low-order finite difference methods are not adequate
- AMR based on rectangles (or cubes) is probably not the most efficient approach
- Two approaches have been shown to be viable:
  - High order finite elements:  $C^0$  vs  $C^1$
  - Field aligned coordinates
- Similar considerations for anisotropy in mass diffusion and wave propagation

# Approach

- Use high-order, *high-continuity* triangular finite elements in poloidal plane, spectral in the toroidal direction
- The compactness and high-continuity of this representation makes a full *implicit* solution practical: including whistler, gyroviscous, and kinetic Alfvén waves

# Divide domain into triangular regions: represent solution as a quintic polynomial within each region



k	$m_k$	$n_k$
1	0	0
2	1	0
3	0	1
4	2	0
5	1	1
6	0	2
7	3	0
8	2	1
9	1	2
10	0	3
11	4	0
12	3	1
13	2	2
14	1	3
15	0	4
16	5	0
17	3	2
18	2	3
19	1	4
20	0	5
21	4	1

The function and its first and second derivatives at the 3 nodes are the global unknowns (6 per node)  $(\phi, \phi_x, \phi_y, \phi_{xx}, \phi_{xy}, \phi_{yy})$

18 constraints to match the function and derivatives at nodes

+ 3 constraints on quintic coefficients to enforce  $C^1$  continuity at edges

21 coefficients of the quintic polynomial

Error  $\sim h^5$  (since complete Taylor series through  $h^4$ )

$C^1$  continuity allows treatment of 4<sup>th</sup> spatial derivatives (Galerkin Method)

Most compact representation for this accuracy “reduced quintic”

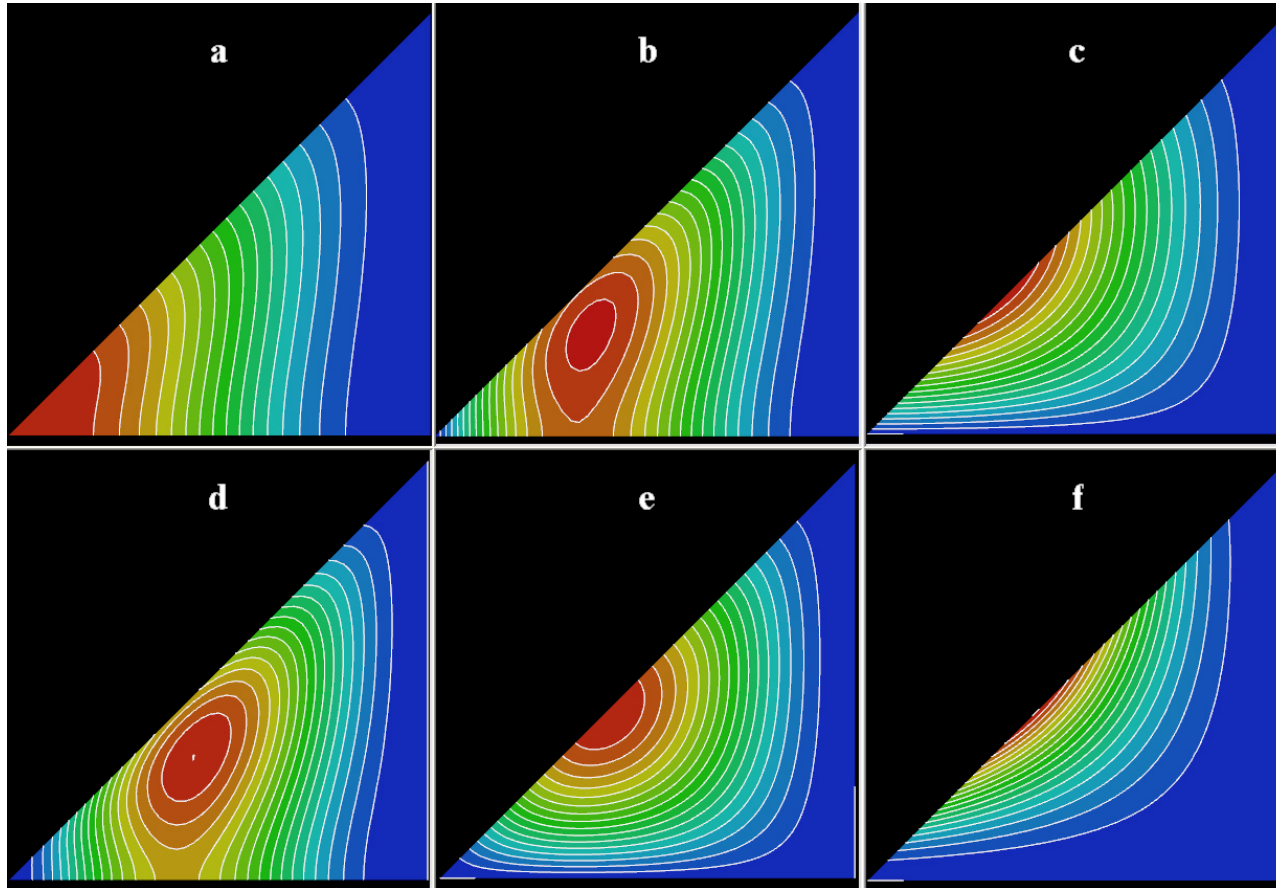


$$a_i = g_{ij} \Phi_j$$

# The Trial Functions:

$$\phi = \sum_{i=1}^{21} a_i \xi^{m_i} \eta^{n_i} = \sum_{i=1}^{21} \sum_{j=1}^{18} g_{ij} \Phi_j \xi^{m_i} \eta^{n_i} = \sum_{j=1}^{18} v_j \Phi_j$$

$$v_j = \sum_{i=1}^{21} \xi^{m_i} \eta^{n_i} g_{ij}$$



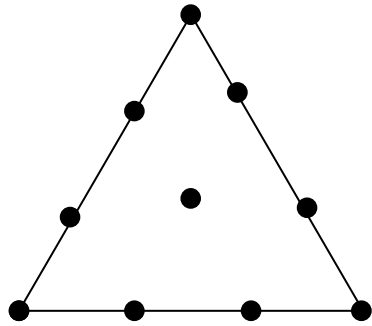
These are the trial functions. There are 18 for each triangle.

The 6 shown here correspond to one node, and vanish at the other nodes, along with their derivatives

Each of the six has value 1 for the function or one of it's derivatives at the node, zero for the others.

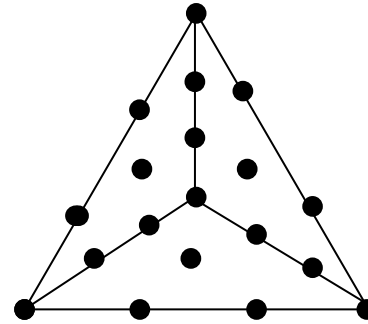
Note that the function and it's derivatives (through 2<sup>nd</sup>) play the role of the amplitudes

# Comparison with a popular $C^0$ Element



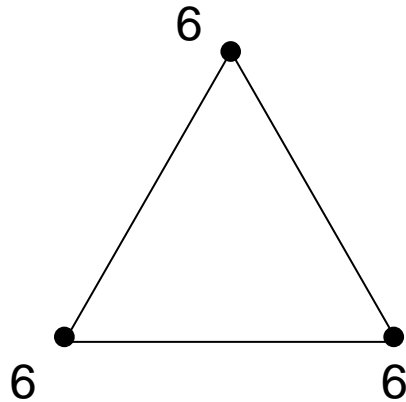
Lagrange Cubic:  $C^0, h^4$

split →



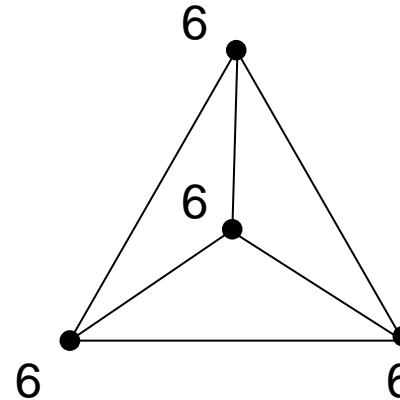
9 new unknowns: 2 new triangles

$9/2 = 4^{1/2}$  unknowns/ triangle



Reduced Quintic:  $C^1, h^5$

split →



6 new unknowns: 2 new triangles

$6/2 = 3$  unknowns/ triangle

# Comparison of reduced quintic to other popular triangular elements

	Vertex nodes	Line nodes	Interior nodes	accuracy order $h^p$	Unknowns per triangle	continuity
linear element	3	0	0	2	$\frac{1}{2}$	$C^0$
Lagrange quadratic	3	3	0	3	2	$C^0$
Lagrange cubic	3	6	1	4	$4\frac{1}{2}$	$C^0$
Lagrange quartic	3	9	3	5	8	$C^0$
reduced quintic	18	0	0	5	3	$C^1$

The “reduced quintic” is the most compact representation of an element of this order of accuracy (fewest unknowns/triangle)

- and -

It's  $C^1$  continuity property allows it to represent spatial derivatives up to 4<sup>th</sup> order without introducing auxiliary variables

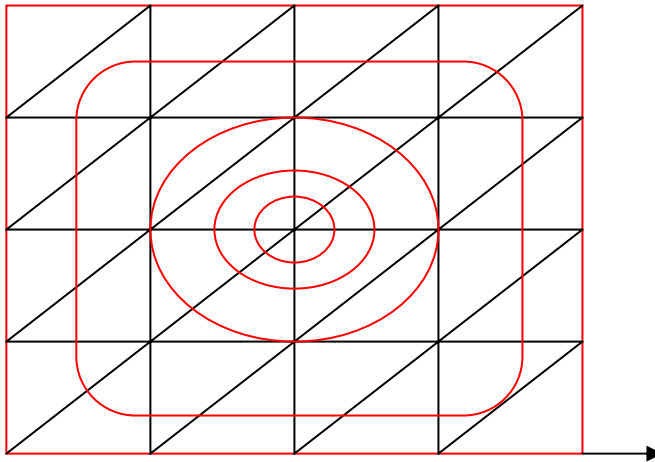
=> Smaller matrices to invert

# Anisotropic Diffusion

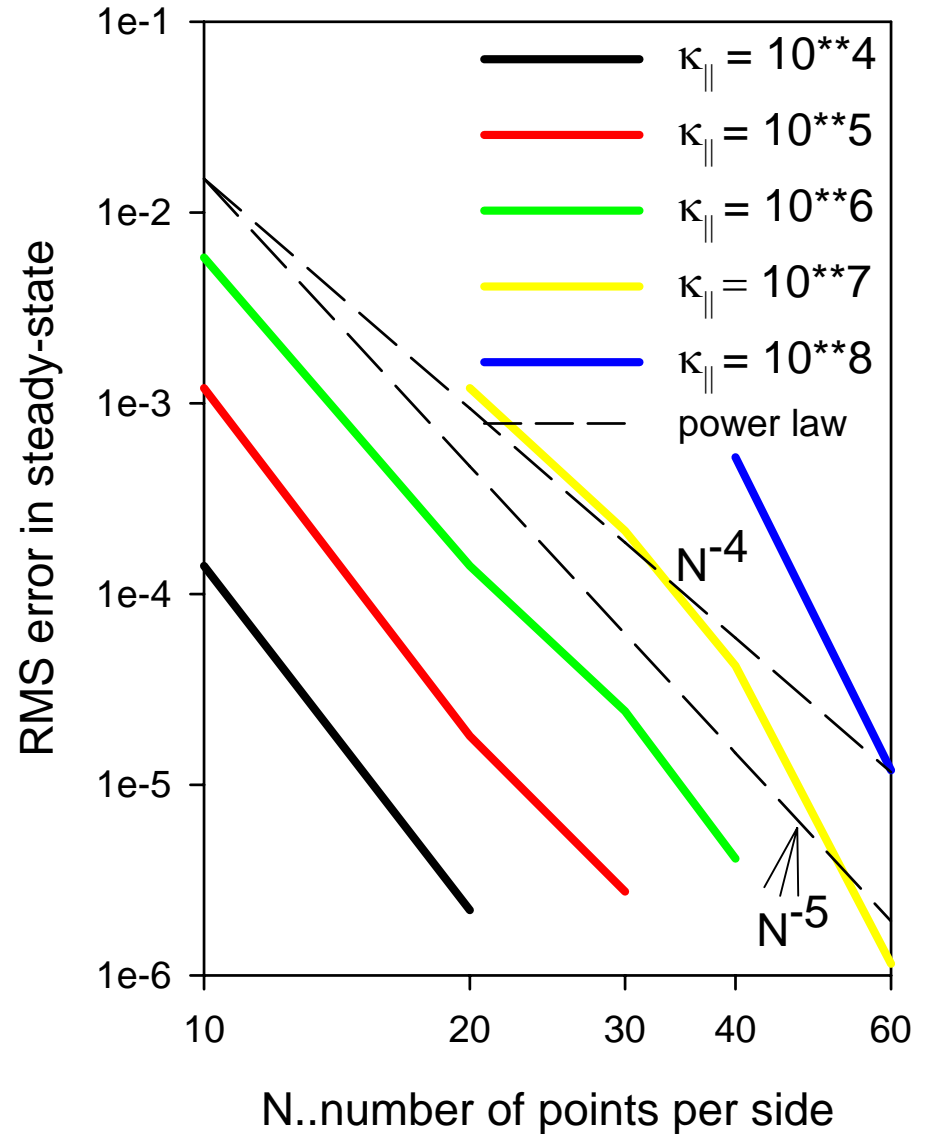
Shows greater than  $N^{-5}$  convergence

$$\frac{\partial \phi}{\partial t} = \nabla \cdot \left[ \kappa_{\parallel} \frac{\vec{B}\vec{B}}{B^2} \cdot \nabla \phi \right] + \nabla \cdot \kappa \nabla \phi + S$$

Solve to steady state



$$S = \psi = \cos \frac{\pi x}{L} \cos \frac{\pi y}{L}$$



# 2D Incompressible MHD

$$\frac{\partial}{\partial t} \nabla^2 \phi + [\nabla^2 \phi, \phi] - [\nabla^2 \psi, \psi] = \mu \nabla^4 \phi$$

$$\frac{\partial \psi}{\partial t} + [\psi, \phi] = \eta \nabla^2 \psi$$

note:

“reduced MHD”

$\phi$  is stream function

$\psi$  is poloidal flux

$[a, b] \equiv \nabla a \times \nabla b \cdot \hat{z}$

$\theta$ -centering.... Taylor expand in time (centered about  $n+1/2$  for  $\theta=0.5$ )

$$\nabla^2 \dot{\phi} + [\nabla^2 \phi^n + \theta \delta t \nabla^2 \dot{\phi}, \phi^n + \theta \delta t \dot{\phi}] - [\nabla^2 \psi^n + \theta \delta t \nabla^2 \dot{\psi}, \psi^n + \theta \delta t \dot{\psi}] = \mu [\nabla^4 \phi + \theta \delta t \nabla^4 \dot{\phi}]$$

$$\dot{\psi} + [\psi^n + \theta \delta t \dot{\psi}, \phi^n + \theta \delta t \dot{\phi}] = \eta [\nabla^2 \psi^n + \theta \delta t \nabla^2 \dot{\psi}]$$

Multiply out non-linear terms, neglecting terms  $\sim (\delta t)^2$ . Finite difference in time:

$$\dot{\phi} = \frac{\phi^{n+1} - \phi^n}{\delta t}, \quad \dot{\psi} = \frac{\psi^{n+1} - \psi^n}{\delta t}$$

Move all terms at time level  $(n+1)$  to left of equal sign. Expand in trial functions. Multiply equations by each trial function and integrate over space. Integrate by parts as needed. (*Galerkin Method*)

$$\phi^n = \sum_{j=1}^{18} v_j \Phi_j^n \quad \psi^n = \sum_{j=1}^{18} v_j \Psi_j^n$$

# Leads to the Matrix Implicit System

$$\begin{bmatrix} S_j^{11} & S_j^{12} \\ S_j^{21} & S_j^{22} \end{bmatrix} \begin{bmatrix} \Phi_j^{n+1} \\ \Psi_j^{n+1} \end{bmatrix} = \begin{bmatrix} D_j^{11} & D_j^{12} \\ D_j^{21} & D_j^{22} \end{bmatrix} \begin{bmatrix} \Phi_j^n \\ \Psi_j^n \end{bmatrix}$$

unknown  
at time n+1

unknown  
at time n

$$\begin{bmatrix} S_j^{11} & S_j^{12} \\ S_j^{21} & S_j^{22} \end{bmatrix} = \begin{bmatrix} A_{i,j} + \theta \delta t [G_{i,j,k} \Phi_k^n - \theta \bar{G}_{i,j,k} \Phi_k^*] & -\theta \delta t \bar{G}_{i,j,k} \Psi_k^* \\ \theta \delta t K_{i,j,k} \Phi_k^n & M_{i,j} + \theta \delta t [K_{i,k,j} \Phi_k^* - \eta A_{i,j}] \end{bmatrix}$$

Block-Sparse coefficient matrices

$$\begin{bmatrix} D_j^{11} & D_j^{12} \\ D_j^{21} & D_j^{22} \end{bmatrix} = \begin{bmatrix} \left\{ \begin{array}{l} A_{i,j} - \delta t [G_{i,j,k} \Phi_k^n - \theta \bar{G}_{i,j,k} \Phi_k^*] \\ \quad + (1-\theta) \mu B_{i,j} \end{array} \right\} & \delta t (G_{i,j,k} \Psi_k^n - \theta \bar{G}_{i,j,k} \Psi_k^*) \\ \delta t K_{i,j,k} (-\frac{1}{2} \Psi_k^n + \theta \Psi_k^*) & \left\{ \begin{array}{l} M_{i,j} - \delta t [K_{i,k,j} (\frac{1}{2} \Phi_k^n - \theta \Phi_k^*)] \\ \quad - (1-\theta) \eta A_{i,j} \end{array} \right\} \end{bmatrix}$$

Solve each time step using SuperLU direct solver

For linear problem, only need to form LU decomposition once and do a back-substitution each time step.

Note that stream function and vorticity are solved together

Each spatial operator becomes a submatrix

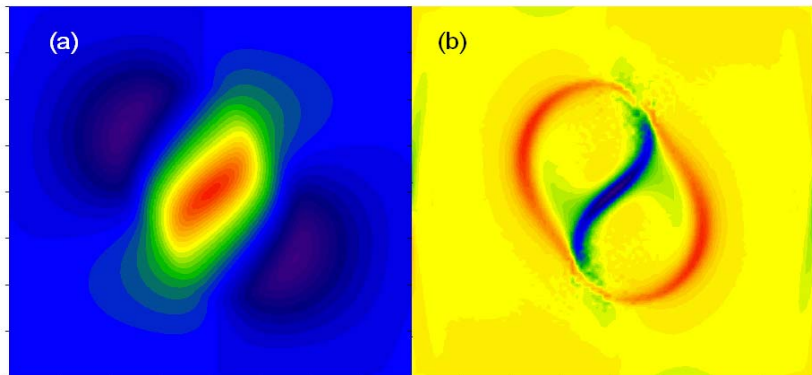
# Tilting of a Plasma Column

Initial Condition:

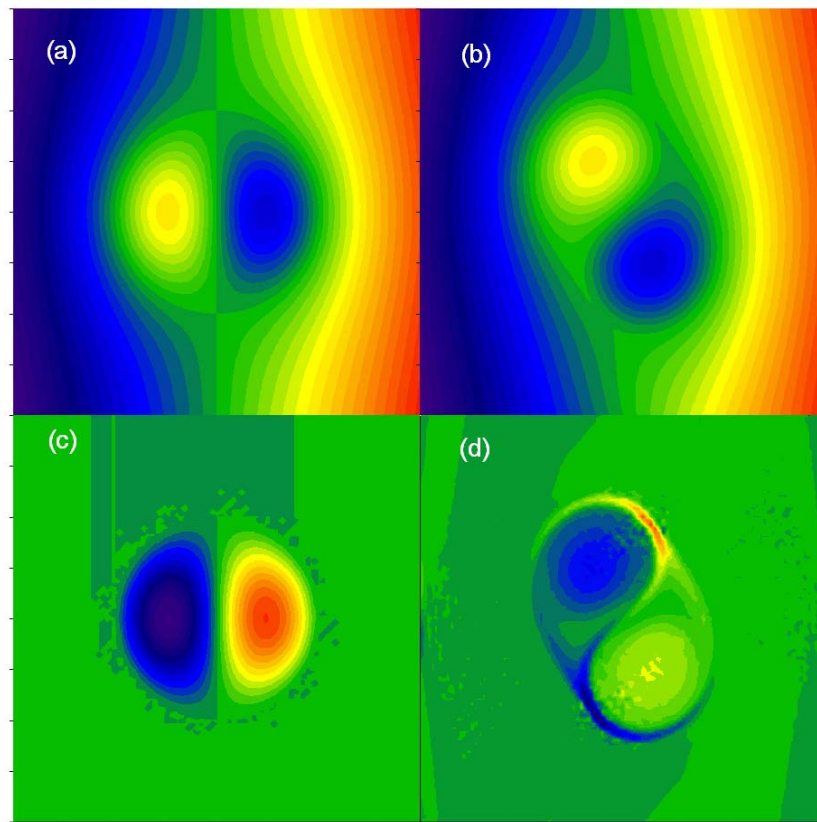
$$\psi = \begin{cases} [2/kJ_0(k)]J_1(kr)\cos\theta, & r < 1 \\ (r - 1/r)\cos\theta, & r > 1 \end{cases}$$

$$J_1(k) = 0$$

Give small perturbation and evolve in time

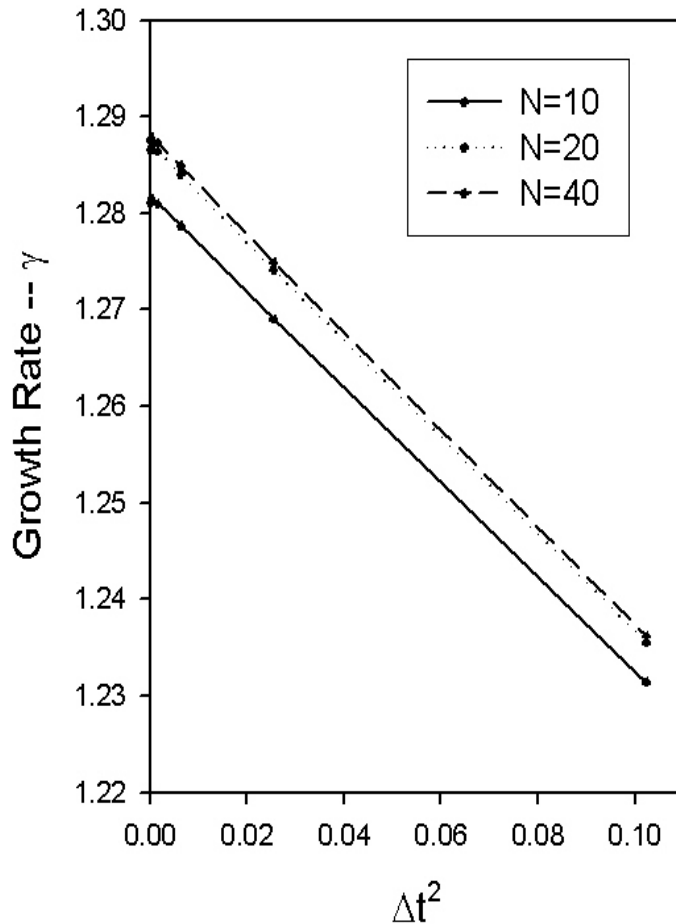


Stream function and vorticity at final time

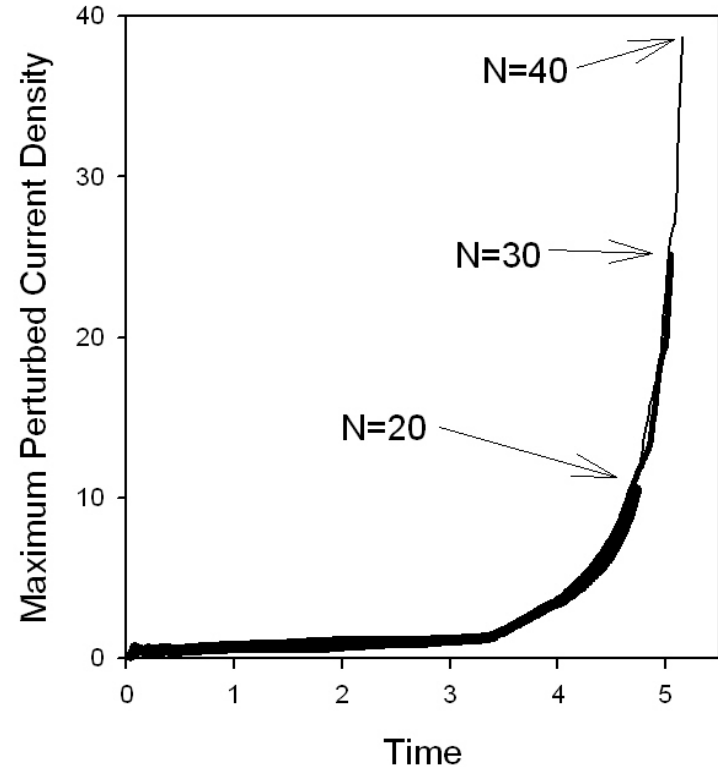


Flux (top) and current (bottom) at initial and final times

# Tilting of a Plasma Column-cont



Converged (in time) growth rate the same for N=30,40 out to 6 decimal places



Calculation stopped each time when energy error reached 1%.



# Higher order formulation

By further manipulation, it is possible to get a 4<sup>th</sup> order (in space) PDE for  $\Phi^{n+1}$  that is independent of  $\Psi^{n+1}$

$$\begin{bmatrix} S_j'^{11} & 0 \\ S_j^{21} & S_j^{22} \end{bmatrix} \begin{bmatrix} \Phi_j^{n+1} \\ \Psi_j^{n+1} \end{bmatrix} = \begin{bmatrix} D_j'^{11} & D_j'^{12} \\ D_j^{21} & D_j^{22} \end{bmatrix} \begin{bmatrix} \Phi_j^n \\ \Psi_j^n \end{bmatrix}$$

Note:

$S_j'^{11}$  now is a 4<sup>th</sup> order operator: contains all the linear Ideal MHD (Alfven wave) response

Instead of inverting full S matrix, invert two sub-matrices sequentially. Gives same results in 1/8<sup>th</sup> – 1/4<sup>th</sup> the time

$$S_j'^{11} \Phi_j^{n+1} = D_j'^{11} \Phi_j^n + D_j'^{12} \Psi_j^n$$

$$S_j^{22} \Psi_j^{n+1} = -S_j^{21} \Phi_j^{n+1} + D_j^{21} \Phi_j^n + D_j^{22} \Psi_j^n$$

M3D-C1 code has full Extended MHD equations expressed in a form that allows non-trivial subsets of lower rank equations:

$$\begin{bmatrix} S_{11}^v & S_{12}^v & S_{13}^v \\ S_{21}^v & S_{22}^v & S_{23}^v \\ S_{31}^v & S_{32}^v & S_{33}^v \end{bmatrix} \cdot \begin{bmatrix} \phi \\ V_z \\ \chi \end{bmatrix}^{n+1} = \begin{bmatrix} D_{11}^v & D_{12}^v & D_{13}^v \\ D_{21}^v & D_{22}^v & D_{23}^v \\ D_{31}^v & D_{32}^v & D_{33}^v \end{bmatrix} \cdot \begin{bmatrix} \phi \\ V_z \\ \chi \end{bmatrix}^n + \begin{bmatrix} R_{11}^v & R_{12}^v & R_{13}^v \\ R_{21}^v & R_{22}^v & R_{23}^v \\ R_{31}^v & R_{32}^v & R_{33}^v \end{bmatrix} \cdot \begin{bmatrix} \psi \\ I \\ T_e \end{bmatrix}^n$$

$$\begin{bmatrix} S_{11}^p & S_{12}^p & S_{13}^p \\ S_{21}^p & S_{22}^p & S_{23}^p \\ S_{31}^p & S_{32}^p & S_{33}^p \end{bmatrix} \cdot \begin{bmatrix} \psi \\ I \\ T_e \end{bmatrix}^{n+1} = \begin{bmatrix} D_{11}^p & D_{12}^p & D_{13}^p \\ D_{21}^p & D_{22}^p & D_{23}^p \\ D_{31}^p & D_{32}^p & D_{33}^p \end{bmatrix} \cdot \begin{bmatrix} \psi \\ I \\ T_e \end{bmatrix}^n + \begin{bmatrix} R_{11}^p & R_{12}^p & R_{13}^p \\ R_{21}^p & R_{22}^p & R_{23}^p \\ R_{31}^p & R_{32}^p & R_{33}^p \end{bmatrix} \cdot \begin{bmatrix} \phi \\ V_z \\ \chi \end{bmatrix}^{n+1} + \begin{bmatrix} Q_{11}^p & Q_{12}^p & Q_{13}^p \\ Q_{21}^p & Q_{22}^p & Q_{23}^p \\ Q_{31}^p & Q_{32}^p & Q_{33}^p \end{bmatrix} \cdot \begin{bmatrix} \phi \\ V_z \\ \chi \end{bmatrix}^n$$

Phase-I: Resistive MHD:

$$\frac{\partial}{\partial t} \nabla^2 \phi + [\nabla^2 \phi, \phi] - [\nabla^2 \psi, \psi] = \mu \nabla^4 \phi$$

$$\frac{\partial \psi}{\partial t} + [\psi, \phi] = \eta \nabla^2 \psi$$

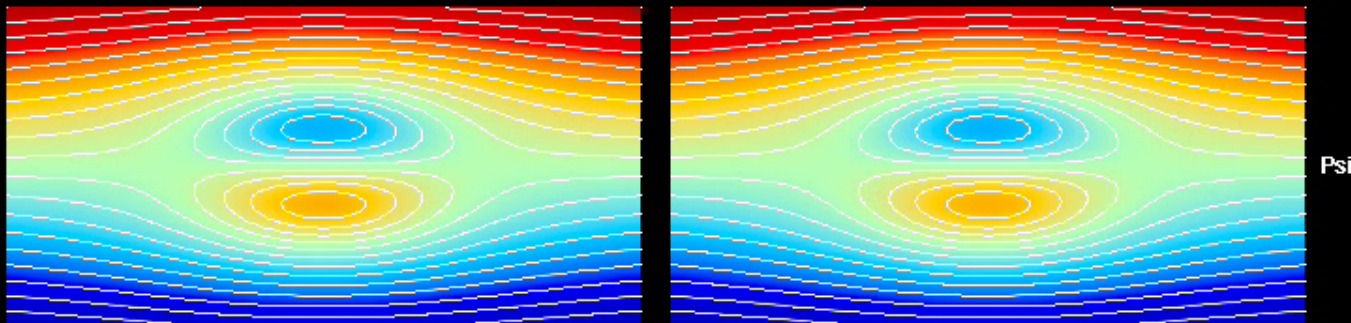
Phase-II: Fitzpatrick-Porcelli 4-field model:

$$\frac{\partial}{\partial t} \nabla^2 \phi = [\phi, \nabla^2 \phi] + [\nabla^2 \psi, \psi] + \mu \nabla^4 \phi$$

$$\frac{\partial V_z}{\partial t} = [\phi, V_z] + c_\beta [I, \psi] + \mu \nabla^2 V_z$$

$$\frac{\partial \psi}{\partial t} = [\phi, \psi] + d_\beta [\psi, I] + \eta \nabla^2 \psi$$

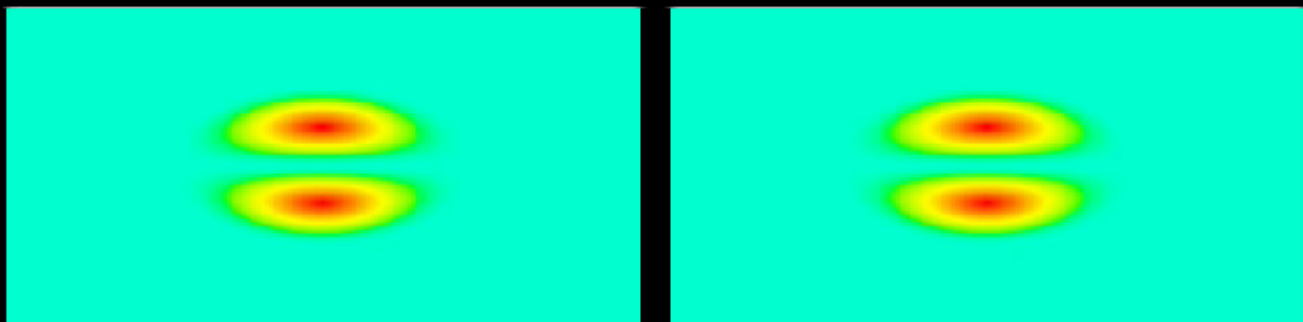
$$\frac{\partial I}{\partial t} = [\phi, I] + d_\beta [\nabla^2 \psi, \psi] + c_\beta [V_z, \psi] + c_\beta^2 \eta \nabla^2 I$$



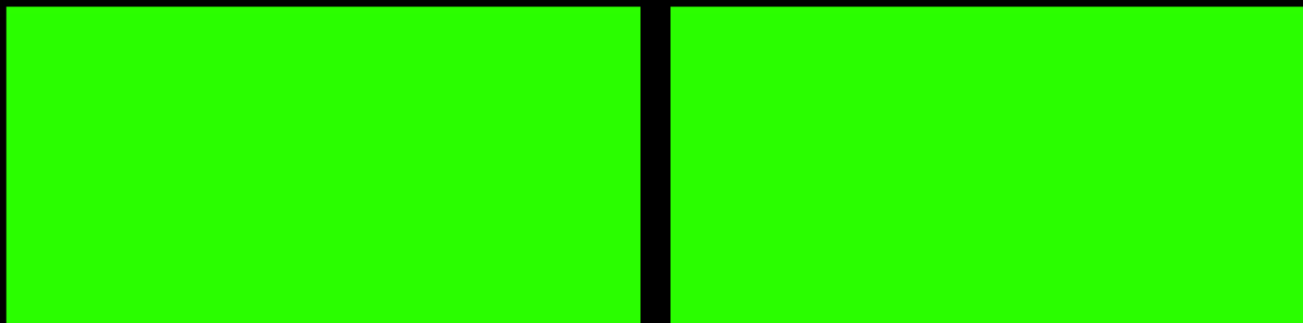
Poloidal  
Magnetic Flux



Toroidal  
Current Density

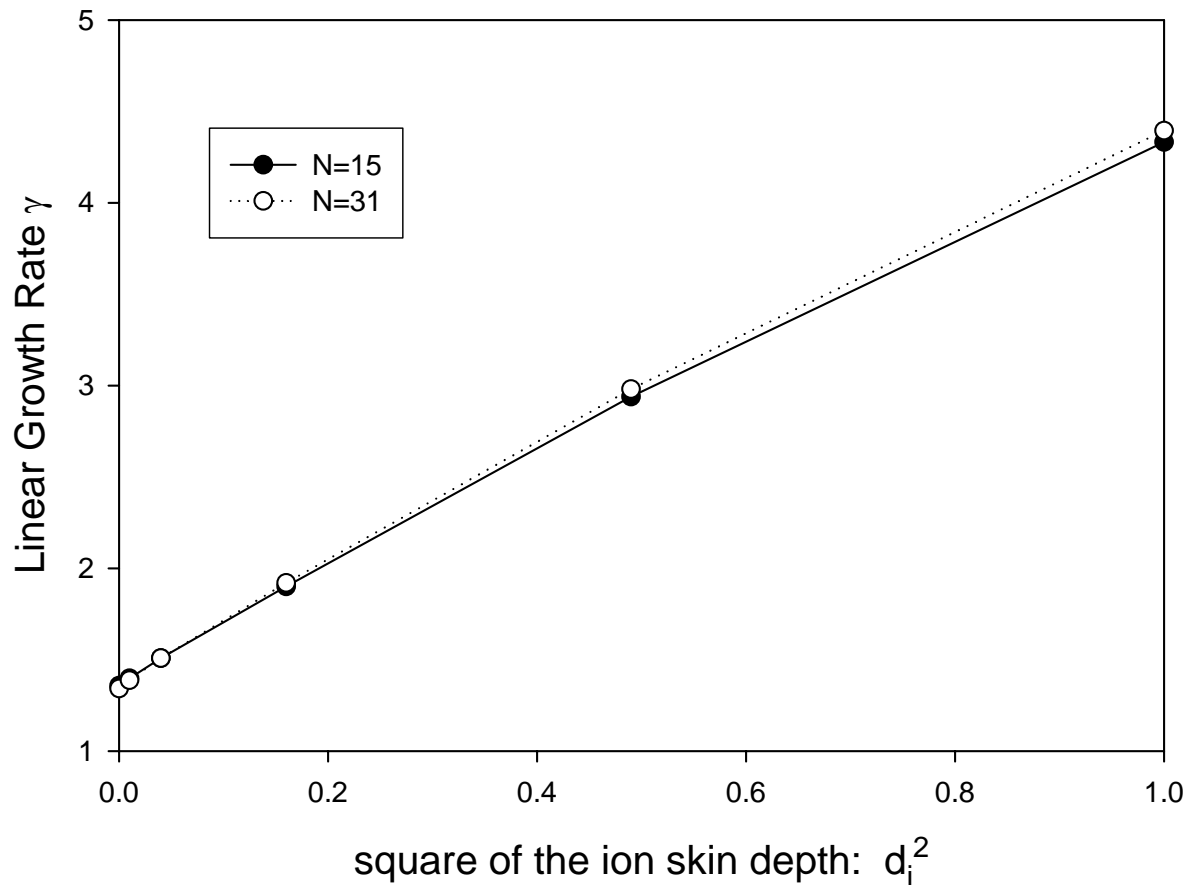


Toroidal  
Magnetic Field

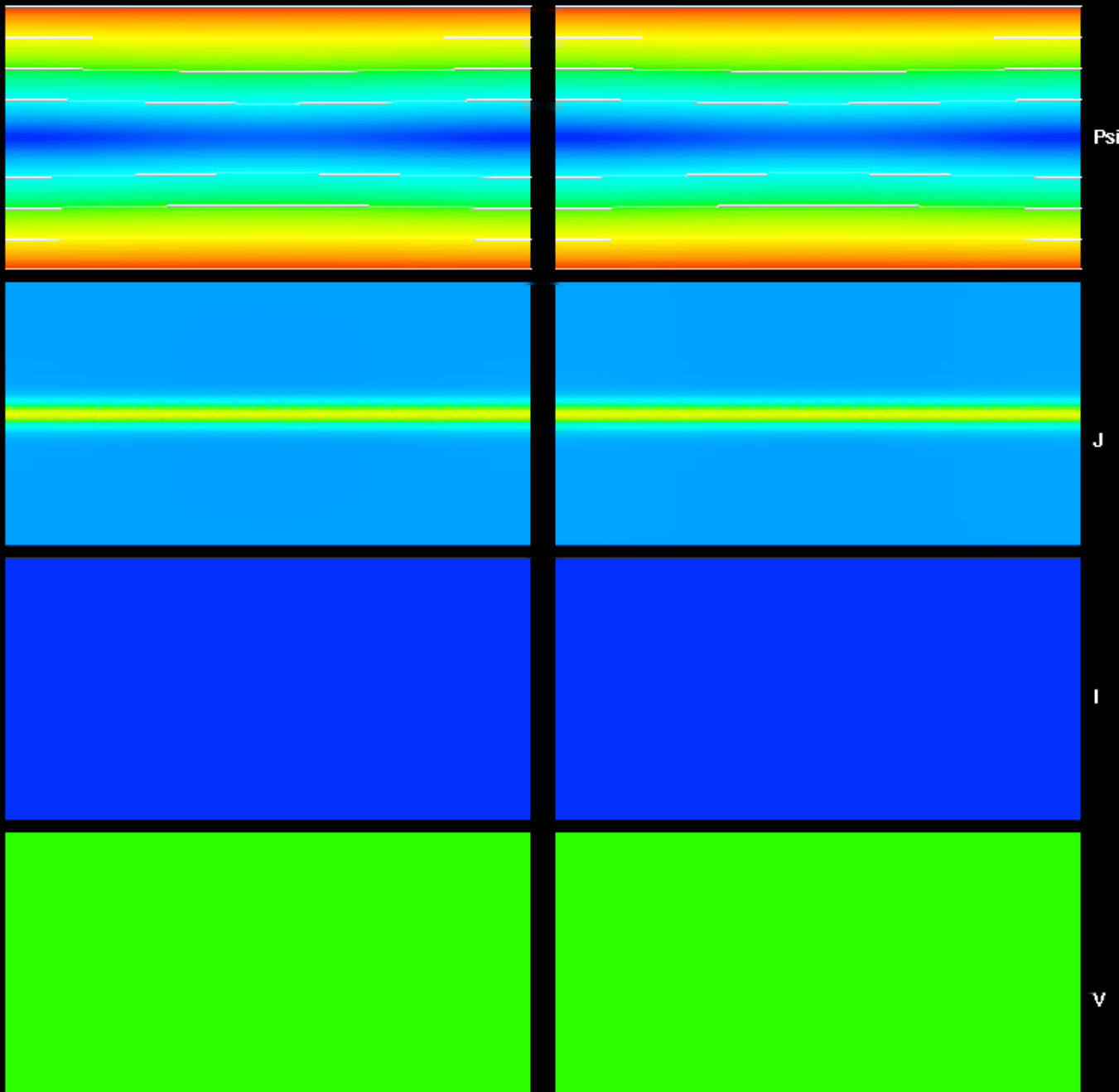


Toroidal  
Velocity

Tilting spheromak in 2-field (left) and 4-field (right) models.



4-field (2-fluid) model predicts that growth rate of tilt mode increases linearly with the square of the ion skin depth  $d_i$



$\Psi$

Poloidal  
Magnetic Flux

$J$

Toroidal  
Current Density

$I$

Toroidal  
Magnetic Field

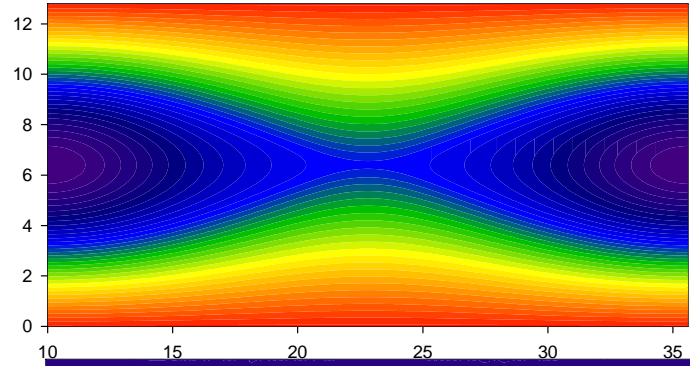
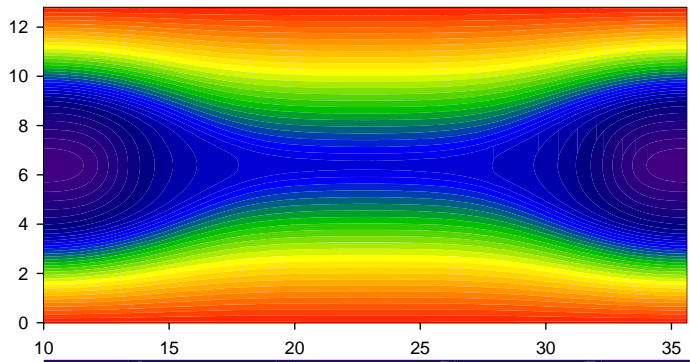
$v$

Toroidal  
Velocity

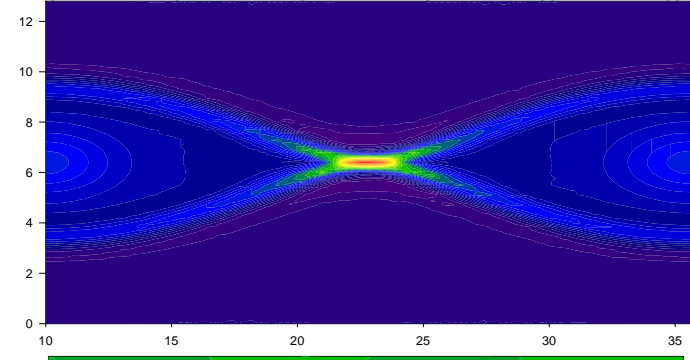
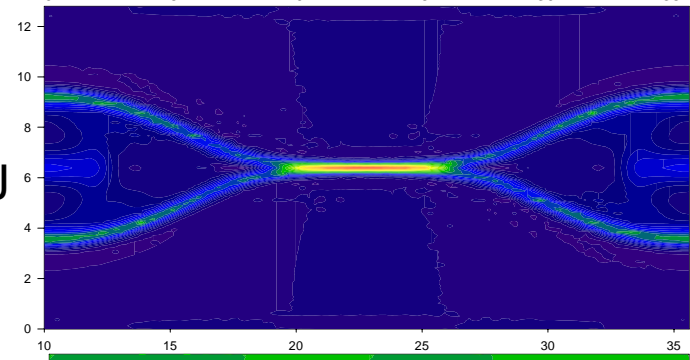
Harris sheet reconnection in 2-field (left) and 4-field (right) models

# Comparison of GEM reconnection with 2-field and 4-field models

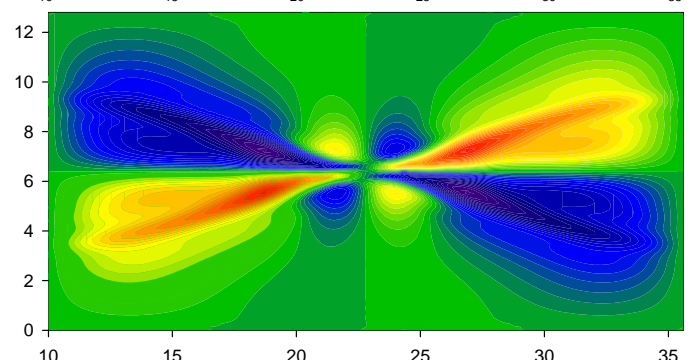
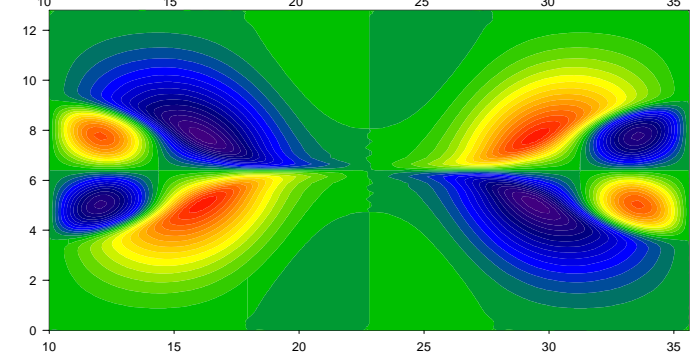
Poloidal Flux  $\Psi$



Current Density  $J$

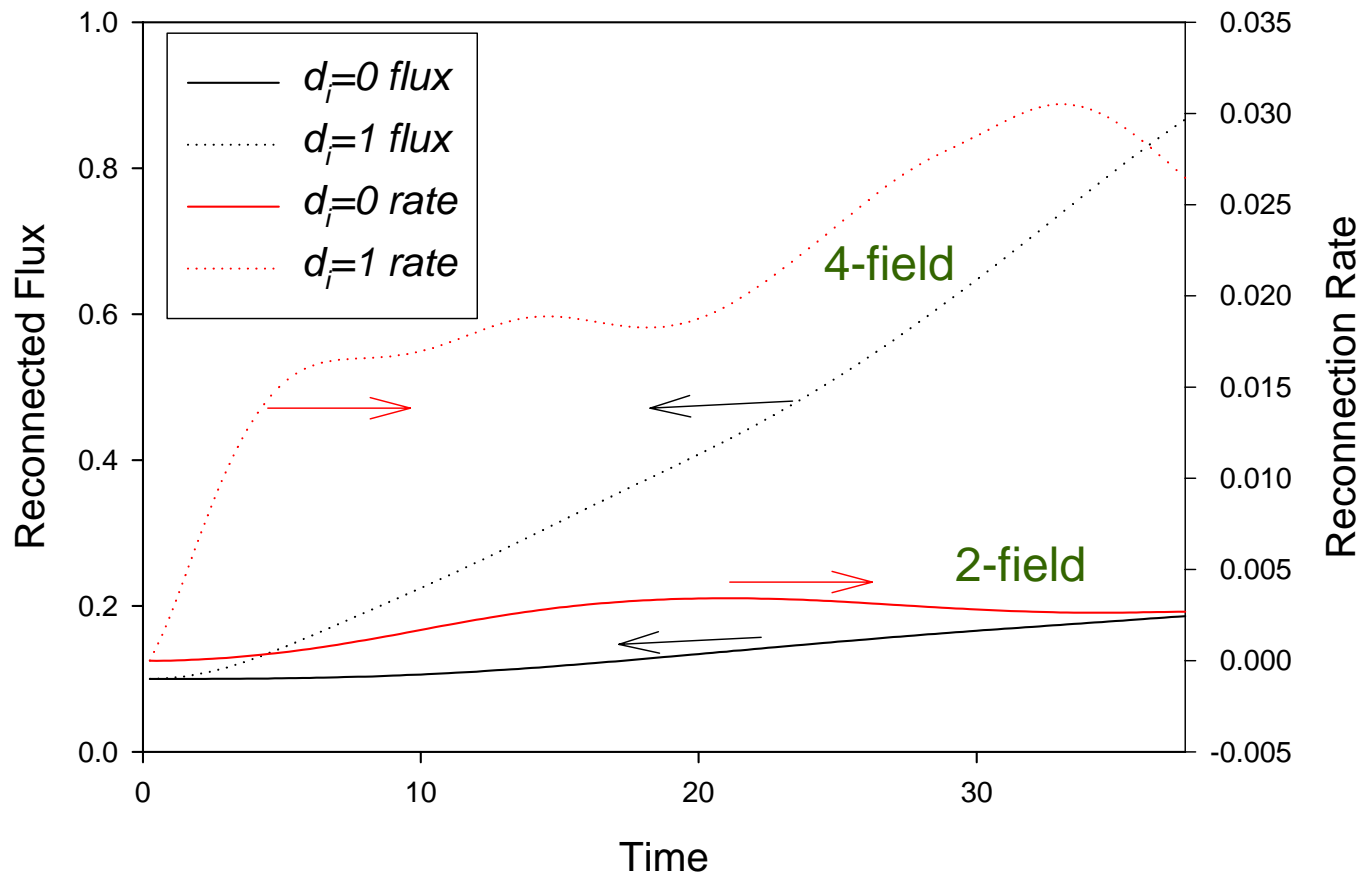


Velocity stream function  $\phi$



2-field reduced resistive MHD

4-field 2-fluid model



4-field (2-fluid) equations with  $d_i=1$  show much greater reconnection rate than 2-field (reduced MHD) description

The 2D cylindrical two-fluid MHD equations and definition of the variables.

$$\frac{\partial \vec{B}}{\partial t} = -\nabla \times \vec{E}$$

$$\vec{V} = \nabla \phi \times \hat{z} + \nabla_{\perp} \chi + v_{\phi}$$

$$\vec{E} + \vec{V} \times \vec{B} = \eta \vec{J} + \frac{1}{ne} (\vec{J} \times \vec{B} - \nabla p_e)$$

$$\vec{B} = \nabla \psi \times \hat{z} + I \hat{z}$$

$$\mu_0 \vec{J} = \nabla \times \vec{B}$$

$$nM_i \left( \frac{\partial \vec{V}}{\partial t} + \vec{V} \cdot \nabla \vec{V} \right) + \nabla p = \vec{J} \times \vec{B} - \nabla \cdot \vec{\Pi}_i^{gv} + \mu n \nabla \cdot [\nabla \vec{V} + \nabla \vec{V}^{\dagger}]$$

$$\frac{\partial n}{\partial t} + \nabla \cdot (n \vec{V}) = 0$$

$$\frac{3}{2} \frac{\partial p_e}{\partial t} + \nabla \cdot \left( \frac{3}{2} p_e \vec{V}_i \right) = -p_e \nabla \cdot \vec{V}_i + \frac{\vec{J}}{ne} \cdot \left[ \frac{3}{2} \nabla p_e - \frac{5}{2} \frac{p_e}{n} \nabla n + \vec{R} \right] - \nabla \cdot \vec{q}_e - Q_{\Delta}$$

$$\frac{3}{2} \frac{\partial p_i}{\partial t} + \nabla \cdot \left( \frac{3}{2} p_i \vec{V}_i \right) = -p_i \nabla \cdot \vec{V}_i - \Pi_i : \nabla V_i + \nabla (\mu n \vec{V}) : [\nabla \vec{V} + \nabla \vec{V}^{\dagger}] - \nabla \cdot \vec{q}_i + Q_{\Delta}$$

$$\frac{3}{2} \frac{\partial p}{\partial t} + \nabla \cdot \left( \frac{3}{2} p \vec{V} \right) = -p \nabla \cdot \vec{V} - \Pi_i : \nabla V_i + \nabla (\mu n \vec{V}) : [\nabla \vec{V} + \nabla \vec{V}^{\dagger}] - \nabla \cdot (\vec{q}_i + \vec{q}_e)$$

$$+ \frac{\vec{J}}{ne} \cdot \left[ \frac{3}{2} \nabla p_e - \frac{5}{2} \frac{p_e}{n} \nabla n + \vec{R} \right]$$



# Numerical stability analysis for 2-fluid equations shows sequential inversion method leads to stability for arbitrary timestep

$$\frac{\partial \vec{V}}{\partial t} = \vec{J} \times \vec{B}_0$$

$$\frac{\partial \vec{J}}{\partial t} = \nabla \times \frac{\partial \vec{B}}{\partial t} = \nabla \times \nabla \times [(\vec{V} - d_i \vec{J}) \times \vec{B}_0] = \vec{B}_0 \times \nabla^2 \vec{V} - d_i \vec{B}_0 \times \nabla^2 \vec{J}$$

$$\dot{V} = -\hat{z} \times \left\{ J + \theta \delta t \left[ \hat{z} \times \nabla^2 (\vec{V} + \theta \delta t \dot{V}) - d_i \hat{z} \times \nabla^2 \vec{J} \right] \right\}$$

$$\dot{J} = \hat{z} \times \nabla^2 \vec{V} - d_i \hat{z} \times \nabla^2 (\vec{J} + \theta \delta t \dot{J})$$

Whistler waves

Alfvén Waves

$$[1 - (\theta \delta t)^2 \nabla^2] (V^{n+1} - V^n) = \delta t \left\{ \theta \delta t [\nabla^2 V^n - d_i \nabla^2 J^n] \right\} - \delta t \hat{z} \times J^n$$

$$[1 + d_i \theta \delta t \hat{z} \times \nabla^2] (J^{n+1} - J^n) = \delta t \hat{z} \times \nabla^2 [\theta V^{n+1} + (1 - \theta) V^n] - d_i \delta t \hat{z} \times \nabla^2 J^n$$

Note: these can be solved sequentially!

Note!

$$\begin{bmatrix} 1 - (\theta \delta t)^2 \nabla^2 & 0 & 0 & 0 \\ 0 & 1 - (\theta \delta t)^2 \nabla^2 & 0 & 0 \\ 0 & \theta \delta t \nabla^2 & 1 & -\theta \delta t d_i \nabla^2 \\ -\theta \delta t \nabla^2 & 0 & \theta \delta t d_i \nabla^2 & 1 \end{bmatrix} \begin{bmatrix} V_x \\ V_y \\ J_x \\ J_y \end{bmatrix}^{n+1} = \begin{bmatrix} 1 - \theta(\theta - 1)(\delta t)^2 \nabla^2 & 0 & -\theta(\delta t)^2 d_i \nabla^2 & \delta t \\ 0 & 1 - \theta(\theta - 1)(\delta t)^2 \nabla^2 & -\delta t & -\theta(\delta t)^2 d_i \nabla^2 \\ 0 & (\theta - 1)\delta t \nabla^2 & 1 & -\delta t d_i \nabla^2 (\theta - 1) \\ -(\theta - 1)\delta t \nabla^2 & 0 & \delta t d_i \nabla^2 (\theta - 1) & 1 \end{bmatrix} \begin{bmatrix} V_x \\ V_y \\ J_x \\ J_y \end{bmatrix}^n$$

# Summary

- Major upgrade to the M3D code is being explored--based on quintic  $C^1$  finite elements
- Primary motivation is to allow efficient, high order, implicit solution of extended MHD equations with whister and KAW
- Staged implementation using reduced sets of equations with 2, 4, and then 6 variables
- Initial results look promising!